Dendrimer Template Directed Self-Assembly during Zeolite Formation

L. Bonaccorsi,[†] D. Lombardo,*[,‡] A. Longo,[§] E. Proverbio,[†] and A. Triolo[‡]

Dipartimento di Chimica Industriale e Ingegneria dei Materiali, Università di Messina, Salita Sperone, 31-98166 S. Agata (Messina), Italy; CNR-IPCF, Istituto per i Processi Chimico Fisici - sez. Messina, C. da Papardo Salita Sperone s.n., I-98158 Messina, Italy; and CNR-ISMN, Istituto per lo studio dei Materiali Nanostrutturati, Sez. Palermo, via Ugo La Malfa 153, I-90146 Palermo, Italy

Received May 30, 2008; Revised Manuscript Received December 29, 2008

ABSTRACT: We describe the formation of a spherical complex driven by the incorporation of aluminosilicate in a dendrimer charged surface. By using a carboxyl-terminated dendrimer species as a macromolecular template for zeolite formation, we detected the formation of porous, stable, and nearly monodisperse spherical aggregates with an average radius of $R = 3500$ Å. The presence of the charge in the surface of the dendrimer, acting as the main driving force, influences the crystallites aggregation as well as the long-range assembly conditions for the zeolite growth. The main finding of our results suggests a possible mechanism for nanoaggregates formation. The dendrimer carboxylate end groups, which are responsible of the long-range electrostatic interparticle interaction, create a diffuse layer of condensed Na^+ ions in the neighborhood of the dendrimer surface which act as the effective structure-directing agent for the zeolite LTA formation. This study put novel insight into the investigation of alternative protocols for the assembly mechanism of porous materials.

Introduction

The fabrication of nanostructured materials for novel technological application can be achieved by exploiting a variety of molecular self-assembly processes.[1] Particularly interesting in this respect is the construction of supramolecular organic−inorganic nanostructured materials based on microporous and nanoporous materials.[2] Zeolites are a class of well-known nanoporous materials largely used in industrial processes as catalysts and adsorbent materials which have recently attracted interest in new applications in agricultural, environmental, and biological technologies.[3,4] Zeolites consist of a cavity network of uniform size nanopores confined within an aluminosilicate or silicate framework. Because of such peculiar structural property, zeolites are able to accommodate specifically sized molecules with long-term chemical and biological stability. In addition, the wide range of framework topologies synthetically available makes zeolites attractive materials for several applications. Zeolites, in general, are obtained by a hydrothermal synthesis in the presence of a template which acts as a structure-directing agent and which is responsible for the final porosity.[5] Particularly stimulating is the study of alternative protocols for the assembly mechanism of such aluminosilicate materials, so-called "template directed assembly", in which some specific macromolecular species (named templates) could drive the formation of aggregate structures with peculiar final properties. The macromolecular species, in this case, promotes specific (noncovalent) interactions that orient the spatial growth of the crystallite assemblies, thus influencing the structural arrangements (size and shape) of the final product. In this way, for example, it could be easier to control the arrangement of the nanosized crystals to grow higher order, defect-free, structures like membranes, films, and coatings. Such self-assembly recently attracted sensitive attention in materials science (such as formation of colloids, molecular crystals, lipid bilayers, and phase-separated polymers) as well as in many processes involved in life sciences.[6] More specifically, the use of branched polymeric materials, such as block copolymers micelles[7] or dendrimers,[8] as nanotemplating agents has been proven as a versatile tool in the field of nanotechnology due to the accurate control of the size and polydispersity of the inorganic particles involved.

Herein, we describe the formation of nanoparticles of zeolite LTA grown on a carboxylate-terminated polyamidoamine (PAMAM) dendrimer. More specifically, we observed that the addition of dendrimers to the synthesis environment modified the crystallites aggregation with a real possibility to affect the long-range assembly conditions for the zeolite growth.

The choice of this macromolecular component relies on the strong condensed cationic Na^+ charge all around the macromolecules, which is responsible for the intense electrostatic interparticle interaction potential.[9,10] In this sense we expect that the Na^+ cation spatial distribution is strongly localized in the vicinity of the dendrimer, thus creating a charged diffuse layer in the neighborhood of the dendrimer surface. We also expect that the condensed Na^+ charge acting as the effective structure-directing agent for the zeolite LTA formation may lead to a condensed growth of the zeolitic phase onto the dendrimer substrate.

Experimental Section

Materials. The zeolite synthesis mixtures, prepared according to the standard procedure,[5,11] had the following molar ratio: 2.0 NaO_2:1 Al_2O_3:1.9 SiO_2:65 H_2O. A further water dilution of the mixture (of about factor 10) has been performed in order to slow down the relevant self-assembly process. PAMAM dendrimers of generation $G = 3.5$ ($M_w = 12\,420$ g/mol) were purchased from Sigma Aldrich and consist of a tetrafunctional ethylenediamine core [⟩NCH_2CH_2N⟨] and [$-CH_2CH_2(C{=}O)NHCH_2CH_2N$⟨] spacers and terminated at the final generation with 64 sodium carboxylate terminal groups (COO^-Na^+) on average. The dendrimers were dispersed in deionized water, while the obtained solutions were filtered with Teflon filters (filter diameter was $D = 0.02$ μm). The solutions were also checked by dynamic light scattering prior to SAXS measurements to remove the presence of possible aggregates in the system. All alluminosilicate reactants were preliminarily mixed and then added with a water solution of generation $G = 3.5$ PAMAM demdrimers at the concentration of $c = 1\%$ w/w [AS/Pamam]. In a clear solution system no gel formation is visible to the naked eye due to the high reactants

* Corresponding author. E-mail: lombardo@me.cnr.it.
[†] Università di Messina.
[‡] Istituto per i Processi Chimico Fisici - sez. Messina.
[§] Istituto per lo studio dei Materiali Nanostrutturati.

10.1021/ma802393e CCC: $40.75
Published on Web 01/22/2009

dilution, so the usual formation of polycrystalline aggregates observed in zeolite grown from a dense gel is largely slowed down.

Light Scattering. Quasi-elastic light scattering (QELS) measurements were carried out at the scattering angle of $\theta = 90°$ using a Brookhaven instrument equipped with a diode laser at a power $P = 35$ mW and with wavelength $\lambda = 661$ nm as exciting source. The collected normalized intensity autocorrelation function $g_2(k,t) = \langle I(k,0)I(k,t)\rangle/\langle I(k,0)\rangle^2$ (being the exchanged wave vector $k = [(4\pi n)/\lambda] \sin(\theta/2)$, where n is the refractive index of the sample) has been analyzed assuming a Gaussian statistics for the scattered electric fields. This last circumstance allows to write the intensity autocorrelation function according to Siegert's relation $g_2(k,t) = 1 + a|g_1(k,t)|^2$, where $g_1(k,t) = \langle E^*(k,0)E(k,t)\rangle/\langle I(k,0)\rangle$ is the normalized scattered electric field $E(k,t)$ autocorrelation function and a is a constant that depends on the experimental setup.[12,13]

Small-Angle X-ray Scattering. The small-angle X-ray scattering (SAXS) patterns have been recorded by a laboratory instrumentation consisting of a Philips PW X-ray generator (providing Cu Kα, Ni-filtered X-ray radiation of wavelength 1.5418 Å) with a Kratky-type small-angle camera in the "finite slit height geometry" equipped with a step scanning motor and scintillator counter as detector. The range of scattering vectors covered is $0.005\ \text{Å}^{-1} < q < 0.4\ \text{Å}^{-1}$. All measurements were carried out at the temperature of $T = 23$ °C. The scattering data were normalized with respect to transmission and were corrected by the empty cell and solvent contribution. Best-fit analysis was performed using homemade programs based on the CERN minimization procedure MINUITS.

Scanning Electron Microscopy. Electron microscopy was performed using a scanning electron microscope (JEOL 5600LV) operated at 10 kV in low-vacuum conditions. The microscope was equipped with a backscattered electron detector and an EDS electronic microprobe (SEMQuant Oxford). Samples of the reactant solution were left to dry overnight at room temperature and then gathered on specimen stubs and submitted to the analysis.

Results and Discussion

Spherical nanometric assemblies were formed when the charged terminal groups of the dendrimer interacted with the aluminosilicate components to irreversibly anchor the zeolite formation to the dendrimer surface. The formation of stable nanoparticles at room temperature was detected 3 h after the dendrimer solution mixing by dynamic light scattering (DLS) experiments, as reported in Figure 1. The analysis of the scattered intensity correlation function[12] for the AS/PAMAM system shows two main relaxation rates indicating the presence of two main populations of particles characterized by different dimensions.

To obtain useful information from the two relaxation modes, a double-exponential fit of the experimental intensity correlation function has been performed, according to the equation[12,13]

$$g^{(1)}(t) = A_F \exp(-k^2 D_F t) + A_S \exp(-k^2 D_S t) \qquad (1)$$

The corresponding diffusion coefficients D_F (fast relaxation) and D_S (slow relaxation) have been used to calculate the particles average hydrodynamic radius from the Stokes−Einstein relation $D = k_B T/6\pi\eta R_H$ (where k_B is the Boltzmann constant, T is the absolute temperature, and η is the solvent viscosity). A summary of the obtained results is presented in Figure 1B. Data show how the fast relaxation contribution is related to a population of small particles which have an hydrodynamic radius increasing with time, from $R_{H1} = 23.0$ Å (for solely PAMAM dendrimer in water solution) to $R_{H1} = 26.0$ Å (3 h after mixing), up to $R_{H1} = 33.5$ Å (26 h after mixing). This variation in particle dimensions may be correlated to the growth of the zeolitic phase onto the charged dendrimer surface. The slow relaxation mode, on the other hand, corresponds to the presence of nearly monodisperse aggregates with an average radius of $R_{H2} = 3500$ Å, which remain rather stable as a function of time (see inset in Figure 1B).

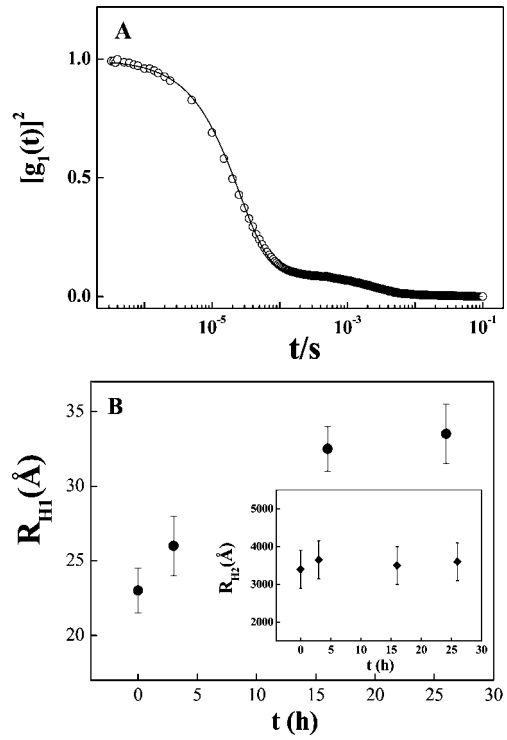

Figure 1. Analysis of the scattered intensity correlation function for the AS/PAMAM system at $T = 25$ °C at an elapsed time of 3 h after the mixing. The two relaxation modes, analyzed according a double-exponential fit of eq 1 (A), correspond to the translational diffusion mode of the two populations of particles with different hydrodynamic radius of R_{H1} (primary units) and R_{H2} (large aggregates). The time behavior of R_{H1} and R_{H2} is reported in (B).

The intensity correlation function $g^1(t)$ obtained from the scattering experiments may also be expressed as the Laplace transform of a continuous distribution $G(\Gamma)$ of decay times (relaxation rates Γ). This allows the calculation of relaxation time distributions $\tau A(\tau) = \Gamma G(\Gamma)$ by means of a regularized inverse Laplace transformation.[14]

$$g^1(t) = \int_0^\infty G(\Gamma) \exp(-\Gamma t)\, d\Gamma = \int_0^\infty \tau A(\tau) \exp\left(-\frac{t}{\tau}\right) \ln \tau \qquad (2)$$

The analysis of the relaxation time distribution $\tau A(\tau)$, performed by using the inverse Laplace transformation algorithm REPES,[14] has been reported as a function of the hydrodynamic radius of the aggregates R_H (Figure 2). This representation confirms that a given distribution of large aggregates is present in the systems in equilibrium with smaller units.

The self-assembly process during nanoparticles formation has been investigated also by means of small-angle X-ray scattering (SAXS) experiments.

For a system composed of nearly monodisperse particles in solution the SAXS scattering intensity $I(q)$ can be expressed as a product of the form factor $P(q)$, which contains information on the shape and dimension of the scattering particles and the structure factor $S(q)$ describing the interparticle interaction[15]

$$I(q) = N(\Delta\rho)^2 P(q) S(q) \qquad (3)$$

where N is the number density of the particles and $\Delta\rho = \rho - \rho_0$ is the so-called "contrast" (i.e., the difference between the scattering length density of the particle ρ and that of the solvent ρ_0). Figure 3 shows the SAXS intensity profile for the G3.5 PAMAM dendrimers in water solution at the three different

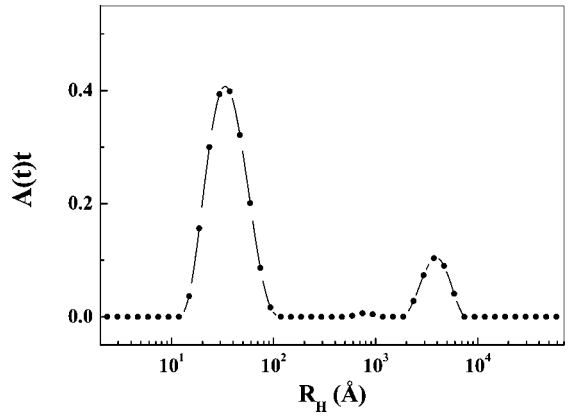

Figure 2. Analysis of the relaxation time distribution $\tau A(\tau)$ obtained by the inverse Laplace transformation of a continuous distribution $G(\Gamma)$ of decay times Γ. The obtained relaxation time distributions, reported as a function of the hydrodynamic radius of the aggregates R_H, indicate the presence of two main populations of aggregates with different dimensions.

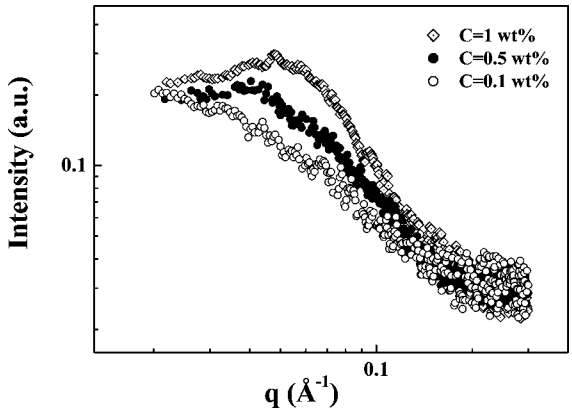

Figure 3. SAXS intensity profile of G3.5 polyamidoamine dendrimers in water solution at three different concentrations in the dilute regime ($C = 1$ wt %, hollow diamonds; $C = 0.5$ wt %, full circles; $C = 0.1$ wt %, hollow circles).

concentrations of $C = 1$ wt %, $C = 0.5$ wt %, and $C = 0.1$ wt %. It is worth noticing that the presence a pronounced structure factor peak for the samples at concentration of $C = 1$ wt % and $C = 0.5$ wt % can be traced back to the sensitive electrostatic interaction caused by the partial ionization of the dendrimers carboxylate surface groups.[9]

In a SAXS experiment, in fact, the static structure factor $S(q)$ can be written as[16]

$$S(q) = 1 + \int_0^\infty 4\pi^2\rho_C[g(r) - 1]\frac{\sin(qr)}{qr}\,dr \qquad (4)$$

where $\rho_C = c/M$ is the particle number density (number of particles per unit volume). This last relation provides a way to connect the structure factor $S(q)$ with the radial pair correlation function $g(r)$ (i.e., the probability that two particles stay at distance r in the system).[16,17] Analysis of the obtained structure factor $S(q)$,[18] presented in Figure 4, confirms the strong inter-dendrimer correlation in solution. More specifically this result state that a sensitive electrostatic repulsion is still present to the average inter-dendrimer distance of d_{ave}=153 Å (for sample at $c = 0.5$ wt %).

In order to obtain direct information on the morphological features of the generated aggregates during nanoparticles formation, the SAXS measurements have been performed 16 h after the mixing of the main aluminosilicate reactants in the presence of the water solution of PAMAM dendrimers at the concentration of $c = 1$ wt % (Figure 5).

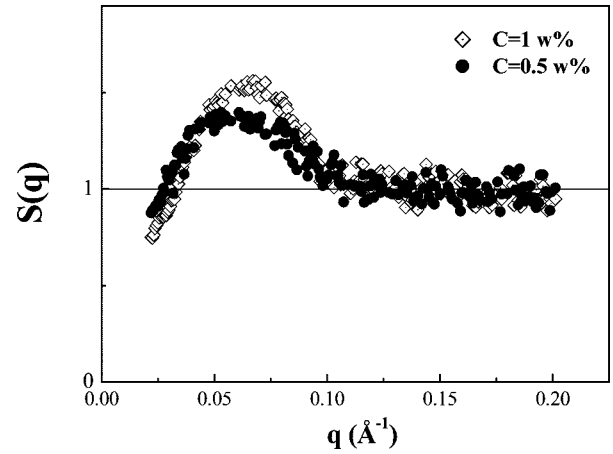

Figure 4. Static structure factor $S(q)$ obtained for two different concentrations in the dilute regime of the generation G3.5 polyamidoamine dendrimers in water solution.

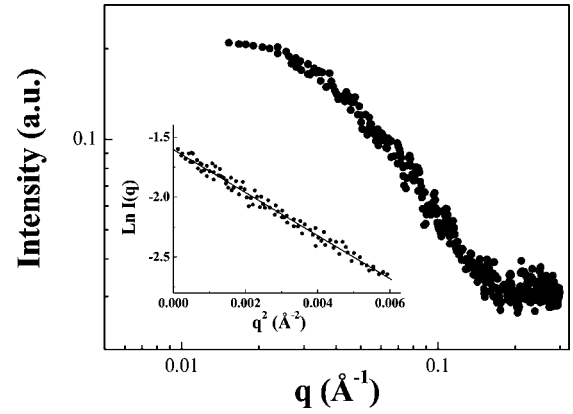

Figure 5. SAXS intensity profile for the AS/PAMAM system 16 h after the mixing of the main components. Guinier fitting analysis of the SAXS intensity profile is given in the inset.

The absence of a peak in the SAXS spectrum clearly indicates that the interparticle interaction can be considered negligible (i.e., $S(q) \approx 1$), and the analysis of SAXS scattering intensity $I(q)$ can furnish information about the form factor $P(q)$.[15] Information about the particle's radius of gyration R_g has been obtained from the slope of the representation ln $I(q)$ vs q^2 in the so-called Guinier region (i.e., for $qR_g \ll 1$), where the particle form factor can be expressed as[15]

$$P(q) = P(0)\exp\left(-\frac{q^2R_g^2}{3}\right) \qquad (5)$$

A radius of gyration of $R_g = 24.6$ Å was obtained from the slope of the representation of ln $I(q)$ vs q^2 (Guinier analysis in the inset of Figure 5) 16 h after the mixing of the main components. A different value of $R_g = 18.9$ Å was obtained for the radius of gyration of solely PAMAM dendrimer in the dilute water solution at the concentration $C = 0.1$ wt %. Both the increase in particle dimensions and the disappearing of the peak in the SAXS spectra may be correlated to the condensed growth of the zeolitic phase onto the charged dendrimer surface. The findings of these results suggests a possible mechanism for nanoaggregates formation. The dendrimer carboxylate end groups, which are responsible for the long-range electrostatic interparticle interaction potential, create a diffuse layer of condensed Na^+ ions in the neighborhood of the dendrimer surface which, acting as the effective structure-directing agent, favor a condensed growth of the zeolitic phase onto the

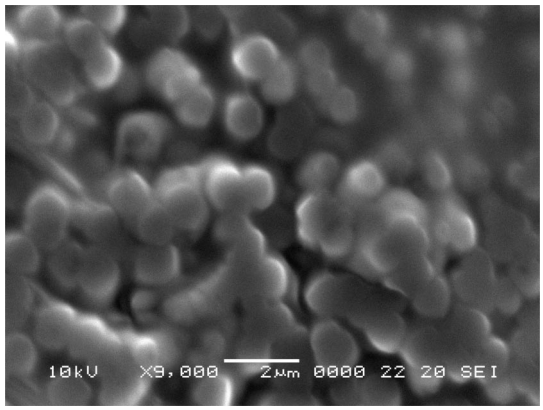

Figure 6. Scanning electron microscopy images of the generated spherical nanostructures for the AS/PAMAM system investigated.

dendrimer substrate. From the morphological point of view, the possibility to obtain core−shell structures for the generated nanoparticles may be less favorable due to the highly ramified nature of the dendrimer core substrate.[19] The growth of the zeolite phase in the interior of the dendrimer, in fact, may be facilitated by possible Na^+ ions migration or by the condensed growth of the zeolite phase into the positively charged amine groups in the interior of the dendrimers. It is worth pointing that although the choice of the dendrimers as a template for porous nanoparticles formation does not ensure a facile removal of the nanotemplate, on the other hand, relevant advantages of the approach rely on the possibility to choice size (i.e., generations) and composition of the template substrate by changing number, typology, or spatial distribution of the interior region components and terminal groups.[19]

The formation of spherical supramolecular assembly at the final stage was finally verified by scanning electron microscopy (SEM) analysis, as shown in Figure 6. The figure shows the presence of, nearly monodisperse, submicron spherical aggregates whose dimensions are compatible with large aggregates previously observed by dynamic light scattering experiments. The backscattered SEM image of the system, 2 days after the mixing, confirmed a condensation of aluminosilicate components on the aggregate surfaces.

Finally, to confirm the nature of the condensate phase, the clear synthesis solution was left reacting at room temperature for 1 week and then was dried at 40 °C for 24 h. The solid was collected and dried again at 80 °C for 12 h and checked by XRD powder diffraction. The analysis of the position of the diffraction peaks of the XRD pattern indicates the formation of crystalline zeolite LTA, thus confirming the porous nature of the generated nanoparticles.

Conclusions

We have demonstrated the successful formation of a spherical complex, driven by the incorporation of aluminosilicate in a dendrimer charged surface. Molecular driving force in this case can be traced back to the strong condensed charge (Na^+ cations from the carboxylic dendrimer terminal groups and from the mother liquid of zeolite components) from the diffuse double layer at the surface of the dendrimer. This condensed charge, acting as an effective structure-directing agent, casted the growth of the zeolite nanoporous structures directly on the dendrimer surface.

The benefits of using a dendrimer nanotemplate for the nanoparticles formation process in zeolite syntheses rely mainly on the possibility to choose size and composition of the core substrate which means driving size and morphology of the condensed surface structures by changing number and typology as well as spatial distribution of the dendrimer terminal groups. The finding of our results may open new perspectives in the synthesis of organic−inorganic nanostructured materials based on mesoporous frameworks with new characteristics and properties. For example, the structural similarities between the substrate-binding sites of enzymes and the zeolites cavities may lead to the development of mesoporous particles capable of mimicking the enzyme functions. Mesoporous barriers, in this case, may be used to promote selective reactions and incorporation of key features of selected enzymes, such as metal complexes. Further investigations of these systems in solution are underway, including time-resolved experiments suitable for a detailed study on the assembly process and to evaluate the effects of the dendrimer chemical structure on nanotemplating reactions.

References and Notes

(1) (a) Corti, M. In *Physics of Amphiphiles: Micelles, Vesicles and Microemulsions*; Degiorgio, V., Corti, M., Eds.; North-Holland: Amsterdam, 1985. (b) Schneider, H.-J.; Yatsimirsky, A. *Principles and Methods in Supramolecular Chemistry*; Wiley & Sons: New York, 2000. (c) Israelachvili, J. *Intermolecular and Surface Forces*; Academic: London, 1991. (d) Lehn, J.-M. *Supramolecular Chemistry: Concepts and Perspectives*; VCH: New York, 1995. (e) Hunter, R. J. *Foundations of Colloid Science*; Oxford University Press: NewYork, 1986; Vols. *I* and *II*.

(2) (a) Velev, O. D.; Tessier, P. M.; Lenhoff, A. M.; Kaler, E. W. *Nature (London)* **1999**, *401*, 548. (b) Breulmann, M.; Davis, S. A.; Mann, S.; Hentze, H. P.; Antonietti, M. *Adv. Mater.* **2000**, *12*, 502–507. (c) Banerjee, S.; Kahn, M. G. C.; Wong, S. S. *Chem.—Eur. J.* **2003**, *9*, 1898–1908. (d) Descalzo, A. B.; Martínez-Máñez, R.; Sancenón, F.; Hoffmann, K.; Rurack, K. *Angew. Chem.* **2006**, *45*, 5924–5948.

(3) Van Bekkum, H., Flanigen, E. M., Jansen, J. C., Eds. *Introduction to Zeolite Science and Practice*; Elsevier: Amsterdam, 1991; Vol. *58*.

(4) Chen, N. Y.; Degnan, T. F., Jr.; Smith, C. M. *Molecular Transport and Reaction in Zeolites, Design and Application of Shape Selective Catalyst*; VCH Publishers: New York, 1994.

(5) (a) Breck, D. *Zeolite Molecular Sieves, Structure, Chemistry and Use*; Wiley: New York, 1974. (b) Barrer, R. M. *Hydrothermal Chemistry of Zeolites*; Academic Press: London, 1982. (c) Barrer, R. M. *Zeolite and Clay Minerals as Sorbents and Molecular Sieves*; Academic Press: New York, 1978.

(6) (a) Chassenieux, C.; Nicolai, T.; Durand, D. *Macromolecules* **1997**, *30*, 4952–4958. (b) He, L.; Garamus, V. M.; Funari, S. S.; Malfois, M.; Willumeit, R.; Niemeyer, B. *J. Phys. Chem. B* **2002**, *106*, 7596–7604. (c) Lafleche, F.; Durand, D.; Nicolai, T. *Macromolecules* **2003**, *36*, 1331–1340. (d) Lombardo, D.; Longo, A.; Darcy, R.; Mazzaglia, A. *Langmuir* **2004**, *20*, 1057. (e) Lombardo, D.; Micali, N.; Villari, V.; Kiselev, M. A. *Phys. Rev. E* **2004**, *70*, 21402–21408. (f) Mazzglia, A.; Angelici, N.; Lombardo, D.; Micali, N.; Patane, S.; Villari, V.; Scolaro, L. M. *J. Phys. Chem. B* **2005**, *109* (15), 7258–7265.

(7) (a) Zhao, D.; Feng, J.; Huo, Q.; Melosh, N.; Fredrikson, G. F.; Chmelka, B. F.; Stucky, G. D. *Science* **1998**, *279*, 548–552. (b) Goltner, C.; Henke, S.; Weissenberger, M. C.; Antonietti, M. *Angew. Chem.* **1998**, *37*, 613–616. (c) Templin, M.; Frank, A.; Chesne, A. D.; Leist, H.; Zhang, Y.; Ulrich, R.; Schadler, V.; Wiesner, U. *Science* **1997**, *278*, 1795–1798.

(8) (a) Gröhn, F.; Kim, G.; Bauer, B. J.; Amis, E. J. *Macromolecules* **2001**, *34*, 2179–2185. (b) Ornatska, M.; Peleshanko, S.; Rybak, b.; Holxmueller, J.; Tsukruk, V. V. *Adv. Mater.* **2004**, *16*, 2206–2211. (c) Juttukonda, V.; Paddock, R. L.; Raymond, J. E.; Denomme, D.; Richardson, A. E.; Slusher, L. E.; Fahlman, B. D. *J. Am. Chem. Soc.* **2006**, *128*, 420–421. (d) Chun, D.; Wudl, F.; Nelson, A. *Macromolecules* **2007**, *40*, 1782–1785.

(9) Micali, N.; Monsu Scolaro, L.; Romeo, A.; Lombardo, D.; Lesieur, P.; Mallamace, F. *Phys. Rev. E* **1998**, *58*, 6229–6235.

(10) Mallamace, F.; Canetta, E.; Lombardo, D.; Mazzaglia, A.; Romeo, A.; Monsù Scolaro, L.; Maino, G. *Physica A* **2002**, *304*, 235–243.

(11) Barrer, R. M. Synthesis of zeolites. In *Zeolites*; Drzaj, B., Hocevar, S., Pejovnik, S., Eds.; Elsevier Science Publishers BV: Amsterdam, 1985.

(12) (a) Berne, B. J.; Pecora, R. *Dynamic Light Scattering*; Wiley-Interscience: New York, 1976. (b) Brown, W. *Light Scattering: Principles and Development*; Clarendon: Oxford, 1996.

(13) (a) Corti, M.; Degiorgio, V. *Phys. Rev. Lett.* **1980**, *45*, 1945–1948. (b) Corti, M.; Degiorgio, V. *J. Phys. Chem.* **1981**, *85*, 711–717. (c) Corti, M.; Degiorgio, V. *Phys. Rev. Lett.* **1985**, *55*, 2005–2008.

(14) (a) Jakes, J. *Czech. J. Phys.* **1988**, *B38*, 1305–1316. (b) Jakes, J. *Czech. Chem. Commun.* **1995**, *60*, 1781–1797.

(15) (a) Feign, L. A.; Svergun, D. I. *Structure Analysis by Small-Angle X-ray and Neutron Scattering*; Plenum Press: New York, 1987. (b) Glatter, O.; Kratky, O. *Small-Angle X-ray Scattering*; Academic Press: London, 1982.

(16) (a) Hansen, J. P.; McDonald, I. A. *Theory of Simple Liquids*; Academic Press: New York, 1986. (b) Hunter, R. J. *Foundations of Colloid Science*; Oxford University Press: NewYork, 1986; Vols. *I* and *III*. (c) Belloni L. In *Neutron X-ray and Light Scattering*; Lindner and Zemb, Eds.; Elsevier Science Publishers B.V.: Amsterdam, 1991.

(17) Waseda, Y. *The Structure of Non-Crystalline Materials*; McGraw-Hill: New York, 1980.

(18) The static structure factor $S(q)$ is obtained by dividing the SAXS intensity profile of the most concentrated systems with the SAXS profile of the sample at concentration of $c = 0.1$ wt %, for which the contribution of the solely form factor $P(q)$ is assumed. Assuming a long-range (liquidlike) order in solution (distorted face-centered-cubic lattice), it is known from the analysis of many simple liquids that the dimensionless product of the first interaction peak, q_{max}, by the mean "nearest neighbor" distance between particles d_{ave}, is a constant quantity given by $d_{ave}q_{max} = k$ (with $k = 1.22(2\pi)$).[16,17] In this respect from the position of q_{max} the value of the average distance between dendrimers can be obtained.

(19) (a) Tomalia, D. A.; Naylor, A. M.; Goddard, W. A. *Angew. Chem., Int. Ed. Engl.* **1990**, *29*, 138–175. (b) Farin, D.; Advinir, D. *Angew. Chem., Int. Ed. Engl.* **1991**, *30*, 1379–1382. (c) Esfand, R.; Tomalia, D. A. *Drug Discovery Today* **2001**, *6*, 427–436. (d) Tomalia, D. A. *Chem. Today* **2005**, *23*, 41–45.

MA802393E